

toxin (*trans*) from 4.7 to 7.2 (*cis*, side pH constant at 4.7) increased G_{ss} from 20- to 50-fold. In cases where a large G_{ss} was already present in symmetric pH solutions, the rate of approach to G_{ss} increased fivefold. In two experiments, returning the *trans* pH to 4.7 reduced the rate of approach to G_{ss} but not its ultimate value. Single-channel "burst" duration and flicker characteristics within a "burst" were unchanged, suggesting that by the scheme presented above the only rate affected would be the unmeasured k_2 (see Fig. 1).

DISCUSSION

These data may have implications for the mechanism of entry of DT into cells. Because imposing a pH gradient across the bilayer modifies the steady-state conductance more than it does the rate of channel opening, the data suggest that pH predominantly affects channel insertion into the bilayer. The undetectable effect of the hydrophilic *A* subunit on the single-channel conductance or "flicker" characteristics of the hydrophobic *B* channel suggests that if the *A* subunit actually crosses the open *B* channel, it might have to do so in an electrically "silent" way, i.e., not clogging the channel for more than several ms. Given that local anesthetics, which are less bulky, cause "flickering" of acetylcholine channel currents in the millisecond timescale (5), the inability to see a new class of short channel flickers with CRM45 makes this explanation less appeal-

ing. A more reasonable hypothesis is that the hydrophilic *A* subunit is folded into the *B* pore during molecular synthesis or membrane insertion, and that the orientation of the inserted toxin is such that *A* merely needs to flip out into the cytoplasm. Is the *B* channel merely a wrapping sleeve left behind after the toxic *A* subunit has popped out?

The inspiration and support of Dr. Alan Finkelstein and the advice of Drs. Bruce Kagan, Harold Lecar, and Robert Guy are gratefully acknowledged.

Received for publication 14 April 1983.

Note added in Proof: An alternative and perhaps more definitive approach to the question posed by this note may be found in the paper by Kagan et al. in this volume.

REFERENCES

1. Pappenheimer, A. M. Jr. 1982. Diphtheria: studies on the biology of an infectious disease. *Harvey Lect.* 76:45-73.
2. Kagan, B. J., A. Finkelstein, and M. Colombini. 1981. Diphtheria toxin fragment forms large pores in phospholipid bilayer membranes. *Proc. Natl. Acad. Sci. USA.* 78:4950-4954.
3. Meyer, D. I. 1982. The signal hypothesis—a working model. *Trends Biochem. Sci.* 7:320-321.
4. Mislser, S. 1983. Gating of ion channels made by a diphtheria toxin fragment in phospholipid bilayer membranes. *Proc. Natl. Acad. Sci. USA.* In press.
5. Neher, E., and J. H. Steinbach. 1978. Local anesthetics transiently block currents through single acetylcholine-receptor channels. *J. Physiol. (Lond.)* 277:153-178.

VIBRATIONAL ANALYSIS OF THE STRUCTURE OF CRYSTALLINE GRAMICIDIN A

VAMAN M. NAIK AND S. KRIMM

Biophysics Research Division, The University of Michigan, Ann Arbor, Michigan 48109

For the channel-forming dimeric species of gramicidin A (GA), single and double-helical structures have been proposed. Single-stranded helical structures are formed by regular intramolecular NH...O hydrogen bonds whereas double helices are formed by the association of two conformationally identical peptide strands wound about a common helix axis and are stabilized by interchain intermolecular NH...O hydrogen bonds. The present x-ray work on GA and its monovalent cation complexes has not been able to distinguish between these two types of structures in the crystalline state (1, 2). The observed dimer chain lengths and channel diameters in both ion-bound and ion-free GA

crystals can be explained by single helical structures dimerized in a head-to-head or tail-to-tail fashion and by parallel or antiparallel double helical structures (3). D,L-alternating oligovalines have been studied recently with regard to their ability to form such helices. One such oligomer, namely Boc-(L-Val-D-Val)_n-OMe, with $n = 4$, is shown to exist in an antiparallel double stranded structure ($\uparrow\downarrow \beta^{5,6}$) by a single-crystal x-ray analysis (4). The x-ray powder diffraction patterns of Boc-(L-Val-D-Val)₆-OMe indicate a similar structure for this compound in the crystalline state (5).

We have studied GA and its Cs⁺ and K⁺ ion complexes and the L,D oligovalines using Infrared (IR) and Raman spectroscopy. Crystals of GA (commercial mixture of gramicidin A, B and C from ICN Life Sciences group, ICN Nutritional Biochemicals, Cleveland OH) and its Cs⁺

This is paper number 20 in a series, "Vibrational Analysis of Peptides, Polypeptides, and Proteins."

and K^+ complexes were grown according to the procedures of references 1 and 2. N-deuterated GA crystals were grown from methanol-D. Raman spectra were recorded using a Spex 1403 double monochromator (Spex Industries, Inc., Metuchen NJ) with an excitation line of 514.5 nm from Ar^+ laser. All spectra were recorded at room temperature using an incident laser power of ~ 100 mW. IR spectra were recorded in KBr disks using a Digilab FTS20C spectrometer (Digilab, Inc., Cambridge, MA) with a resolution of 1 cm^{-1} .

RESULTS AND DISCUSSION

Observed Raman and IR spectra of GA and its Cs^+ complexes are shown in Figs. 1 and 2. Spectra of Cs^+ and K^+ complexes are almost identical. Table I lists the observed amide A, B, I, II, III, and V frequencies of Boc-(L-Val-D-Val) $_8$ -OMe, GA, and its Cs^+ complex in the crystalline state.

Our earlier spectroscopic studies on L, D-oligovalines (6) indicate that Boc-(L-Val-D-Val) $_8$ -OMe has a double helical structure similar to that of Boc-(L-Val-D-Val) $_4$ -OMe. Native GA crystals show amide A, B, I and III modes similar to hexadecavaline. The strongest Raman

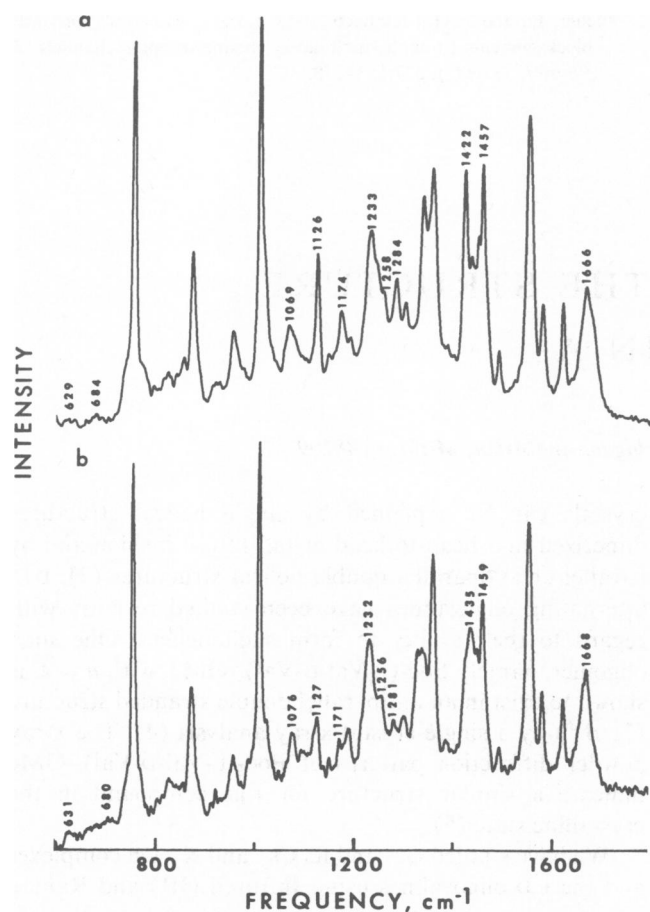


FIGURE 1 Raman spectra in the 600–1,800 cm^{-1} region of (a) native gramicidin A crystals and (b) crystals of Cs^+ -gramicidin A complex.

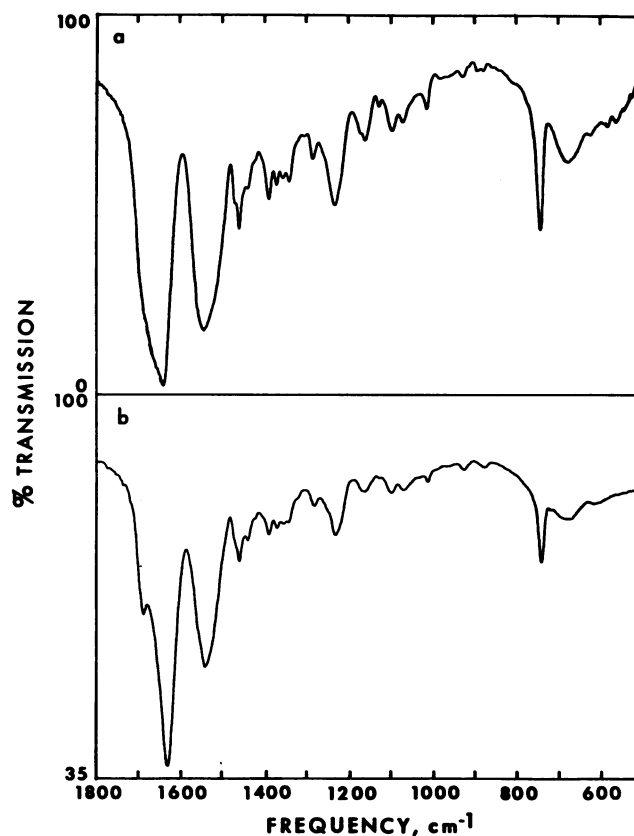


FIGURE 2 Infrared spectra in the 500–1,800 cm^{-1} region of (a) native gramicidin A crystals and (b) crystals of Cs^+ -gramicidin A complex.

amide I mode of GA is $\sim 4\text{ cm}^{-1}$ lower, and the amide II $\sim 10\text{ cm}^{-1}$ lower than that of hexadecavaline. Amide V frequencies of GA are also lower compared to hexadecavaline. All these observations indicate the presence of somewhat weaker hydrogen bonds in GA.

The crystals of cation-bound GA complexes do not show any major differences in the observed IR and Raman spectra in comparison to the native GA crystalline spectra, although there are some subtle differences. Notable differences are downshifting of the IR amide I band by $\sim 8\text{ cm}^{-1}$ and loss of intensity in the Raman 1,422 cm^{-1} and 1,284 cm^{-1} bands. The high-frequency component of amide I observed only as a shoulder in native crystals becomes more prominent in ion-bound GA crystals. Our observed IR frequencies of the Cs^+ complex differ from the ones reported by Iqbal and Weidekamm (7), who reported only the amide A and I modes. The observation of an amide A band at 3,320 cm^{-1} and an additional amide I band at 1,735 cm^{-1} in their study indicates the presence of a nonregular backbone structure. The 1,735 cm^{-1} band indicates a breaking of some hydrogen bonds, and 3,320 cm^{-1} for an amide A is rather high for a hydrogen-bonded NH group.

Lotz et al. (8) have characterized the single and double helical structures formed by poly(γ -benzyl-D-L-glutamate) using IR, x-ray, and electron diffraction studies. Their

TABLE I
AMIDE FREQUENCIES (cm⁻¹) OF Boc-(L-Val-D-Val)₈-OME, GRAMICIDIN A AND GRAMICIDIN-A-Cs⁺

	VAL-16*		Gramicidin A		Gramicidin A-Cs ⁺	
	Raman	IR	Raman	IR	Raman	IR
Amide A	3267 M	3280 S‡	3274 M	3285 S	3280 M	3285 S
Amide B		3075 M		3078 W		3078 W
		1684 sh	1678 sh	~1680sh		1685 M
Amide I	1672 VS		1666 S		1668 S	
		1640 VS		1638 VS		1630 VS
Amide II		1552 S		1542 S		1539 S
			1284 M	1285 W	1279 VW	1280 VW
Amide III	1272 M		1258 W		1256 W	
			1243 sh			
	1230 VS	1231 M	1233 S	1233 M	1233 S	1230 M
	694 VW	700 M	684 W	676 M	698 W	680 M
Amide V			641 VW			
			629 VW	626 W	624 VW	617 VW

*VAL-16 = Boc-(L-Val-D-Val)₈-OME

‡S = strong, M = medium, W = weak, V = very, and sh = shoulder

findings show that all the double helical structures ($\uparrow\downarrow\beta^{5,6}$, $\uparrow\downarrow\beta^{7,2}$, $\uparrow\downarrow\beta^{9,0}$ and $\uparrow\downarrow\beta^{10,8}$) have a strong amide I band at $\sim 1,630$ cm⁻¹ accompanied by a shoulder at $\sim 1,690$ cm⁻¹ and an amide A band at $\sim 3,285$ cm⁻¹. The strongest amide II band is observed at $\sim 1,535$ cm⁻¹. Single-helical structures such as $\beta^{4,4}$ have much higher amide I and II frequencies: $1,645$ cm⁻¹ and $1,557$ cm⁻¹. Amide A for this structure is observed at $3,272$ cm⁻¹. In light of these observations the suggestion of an NH₂-terminal-to-NH₂-terminal helical dimer for GA in dimyristoyl phosphatidylcholine (DMPC) vesicles by Nabadryk et al. (9) does not seem correct. Their suggestion was based on the observed frequencies for amide I at $1,638$ cm⁻¹ and for Amide II at $1,547$ cm⁻¹.

From the literature results and the present study the following conclusions can be drawn. The closeness of the observed spectra in hexadecavaline and the native GA crystals suggests a double helical structure of the type $\uparrow\downarrow\beta^{5,6}$ for the native GA. This is in agreement with the studies of Lotz et al. (8). There are only small spectral differences observed in the cation-bound crystals in the amide frequencies. These frequencies match very well with the observed frequencies in the conventional antiparallel β -sheet structure of poly(L-alanine). These results, along with the observations of Lotz et al. (8), indicate a double-helical structure for GA in the cation-bound crystals. For these crystals a structure of the type $\uparrow\downarrow\beta^{7,2}$ fits the observed dimer chain length and the channel diameter (1, 2). This is also supported by the fact that the ion-bound conformation is the same for the ions Cs⁺, K⁺ and TI⁺, all of which have different ionic radii. The $\uparrow\downarrow\beta^{7,2}$ structure has a channel diameter big enough to hold any of these ions (3). The changes observed in Raman bands at $1,422$ cm⁻¹ (assignable on the basis of deuteration studies to NH in-plane motion of the tryptophan side chain) and $1,174$ and $1,069$

cm⁻¹ (due to C-O-H end group) indicate that the ions are likely to be bound at the COOH-terminus. This possibly means that the cations are bound at 2.5 Å from the ends of the channel. This is one of the two possible sites suggested in the x-ray work (3). Normal modes have been computed for infinite $\beta^{4,4}$, $\beta^{6,3}$, $\uparrow\downarrow\beta^{5,6}$ and $\uparrow\downarrow\beta^{7,2}$ with the side chain approximated by a point mass equal to CH₃. The calculated splittings in amide I are $\beta^{4,4} - 17$ cm⁻¹, $\beta^{6,3} - 11$ cm⁻¹, $\uparrow\downarrow\beta^{5,6} - 39$ cm⁻¹, and $\uparrow\downarrow\beta^{7,2} - 45$ cm⁻¹. The double helical structures predict very well the observed $\sim 1,680$ cm⁻¹ IR frequency whereas single helical structures do not. The $\beta^{6,3}$ structure predicts the lowest amide I frequency at $1,643$ cm⁻¹, in good agreement with the IR studies of Urry et al. (10) on malonyl-bis-desformyl gramicidin (a covalent head to head dimer).

Received for publication 25 May 1983.

REFERENCES

1. Koeppe II, R. E., K. O. Hodgson, and L. Stryer. 1978. Helical channels in crystals of gramicidin A and a cesium-gramicidin A complex: an x-ray diffraction study. *J. Mol. Biol.* 121:41-54.
2. Koeppe II, R. E., J. M. Berg, K. O. Hodgson, and L. Stryer. 1979. Gramicidin A crystals contain two cation binding sites per channel. *Nature (Lond.)* 279:723-75.
3. Chandrasekaran, R., and B. V. V. Prasad. 1978. The conformation of polypeptides containing alternating L and D amino acids. *CRC Crit. Rev. Biochem.* 125-161.
4. Benedetti, E., B. DiBlasio, C. Pedone, G. P. Lorenzi, L. Tomasic, and V. Gramlich. 1979. A double stranded β -helix with antiparallel chains in a crystalline state and in chloroform. *Nature (Lond.)* 282:630.
5. Lorenzi, G. P., L. Tomasic, C. Pedone, and B. DiBlasio. 1983. β -helical structure of Boc-(L-Val-D-Val)₆-OME in the crystalline state and in chloroform. *Helv. Chim. Acta.* 66:158-167.
6. Naik, V., and S. Krimm. 1983. Vibrational analysis of L, D peptides: structural analogues of gramicidin A. *Biophys. J.* 41:(2,Pt.2) (Abstr.).

7. Iqbal, Z., and E. Weidekamm. 1980. Raman and infrared spectroscopic study of gramicidin A conformations. *Arch. Biochem. Biophys.* 202:639-649.
8. Lotz, B., F. Colonna-Cesari, F. Heitz, and G. Spach. 1976. A family of double helices of alternating poly(γ -benzyl-D-L-glutamate), a stereochemical model for gramicidin A. *J. Mol. Biol.* 106:915-942.
9. Nabedryk, E., M. G. Gingold, and J. Breton. 1982. Orientation of gramicidin A transmembrane channel. Infrared dichroism study of gramicidin in vesicles. *Biophys. J.* 38:243-249.
10. Urry, D. W., R. G. Shaw, T. L. Trapane, and K. U. Prasad. 1983. Infrared spectra of the gramicidin A transmembrane channel: the single stranded β^6 -helix. *Biochem. Biophys. Res. Commun.* 114:373-379.

ACTIVATION AND INACTIVATION OF MELITTIN CHANNELS

M. T. TOSTESON AND D. C. TOSTESON

Department of Physiology and Biophysics, Harvard Medical School, Boston, Massachusetts 02115

Melittin, the major toxin of the bee venom, produces a variety of effects on natural membranes, including cell lysis, activation of phospholipase A, antimicrobial activity and alterations in mitochondrial respiration and adenylate cyclase activity (1). We have recently shown that this amphiphilic peptide, which consists of 26 amino acid residues, including six with positively charged side chains, induces a voltage-dependent conductance in lecithin (asolectin) bilayers (2). The present communication describes in detail the temporal course of this conductance induced by melittin.

MATERIALS AND METHODS

All salts used were reagent grade. Melittin was either purchased from Sigma Chemical Co. (St. Louis, MO) or kindly provided by Dr. S. C. Quay. Bilayers were made from asolectin (Associated Concentrates, Long Island, NY) by apposition of two monolayers (3). The area of the films ranged from 0.05×10^{-2} to 1.3×10^{-2} cm². The aqueous solutions contained unbuffered 1 M NaCl. Melittin was added to one aqueous compartment (*cis*) as small aliquots of a concentrated ethanolic solution. The final ethanol concentration was always less than 1%.

Currents were measured using a fast-settling, high input impedance amplifier (LF157A, National Semiconductors), DC pulses of varying amplitude and duration were applied using a programmable function generator (model 5900, Krohn-Hite Co., Avon, MA). The sign of the potential refers to the compartment to which melittin was added. Positive charge flowing from the *cis* to the *trans* compartment is plotted as positive (upward) current.

RESULTS AND DISCUSSION

Fig. 1 *A* shows the temporal course of the current across an asolectin bilayer in response to a step in voltage. The first fast rise in current (*a*) is depicted with better time resolution in panel 1 *B*, where it is seen that this first current increase shows activation that reaches a steady-state ($dI/dt = 0$) with a half-time of 0.5 to 2 ms. The current-voltage (*I-V*) curve of the steady-state current, shown in Fig. 2 *A*, yields the ($\lg G$)-*V* curve shown in 2 *B*. From these curves it is possible to calculate that the conductance changes *e*-fold/16-20 mV change in the applied potential. Also

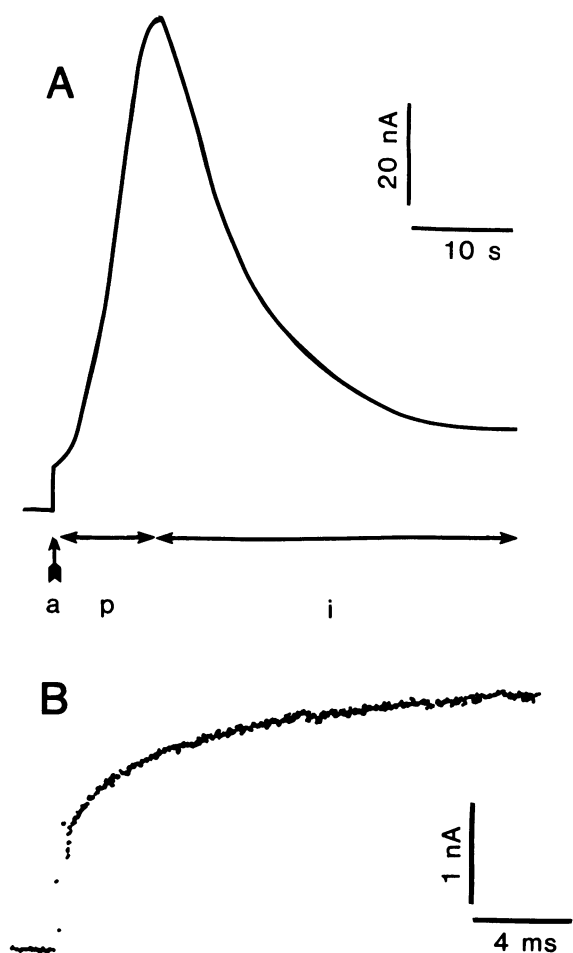


FIGURE 1 Time course of the current response to a constant voltage pulse. *A*, current response to a step in voltage. The +62 mV pulse was started at the arrow and was maintained through the region labeled *i*. *B*, current response to a step in voltage of short duration. 30 pulses of 20 ms duration and +62 mV amplitude were applied to the bilayer with a frequency of 10 Hz before the sequence shown in panel *A* was obtained. The individual current responses were added in a signal averager, after compensation for the bilayer capacitance. Melittin concentration (*cis*-side only): 1.5×10^{-7} M.